Integrating Net Benefits Test for Demand Response Into Optimal Power Flow Formulation

Jessie Ma, *Member, IEEE*, and Bala Venkatesh, *Senior Member, IEEE*

***Abstract*—In 2011, the Federal Energy Regulatory Commission (FERC) mandated that demand response (DR) procurement pass a net benefits test (NBT) in Order 745 to ensure that the benefits outweighed the costs. Without NBT, DR procurement could result in losses to consumers considering payments for energy and DR services. Current NBT implementations are monthly. However, this neglects to consider two important issues: (a) generator supply curve and demand changes on an hourly basis thus altering the maximum DR quantity that can be dispatched considering NBT; and (b) system-wide implementations don't consider locational marginal prices, line flow limits, and network congestion. Both of these issues can severely distort proper implementation of the NBT. However, FERC allowed the NBT be applied monthly and system-wide in recognition of computational difficulties and lack of methods, and FERC called for research in real-time implementations of NBT. Our work responds to this call. To address these two shortcomings, we propose a new optimal power flow (OPF) formulation in which NBT is implemented into a real-time or near real-time dispatch OPF model and considers the network model in its entirety. Our proposed methodology is applied to a 4-bus test system, a 118-bus modified IEEE system, and a real Ontario system. We demonstrate that the embedding of NBT into real-time OPF formulation yields maximum benefits to remaining consumers when compared to conventional DR formulations.**

***Index Terms*—Electricity markets, Optimal power flow, Demand Response.**

NOMENCLATURE

A. Indices

$i,\ j$	Bus indices
q	Term index of objective function
k	Line index
l, m, n	Neural network neuron indices for Layers 3, 2, and 1 respectively

B. Parameters

NB	Total number of buses
NQ	Number of terms in the objective function
KD_i	Demand bid price at bus i
KG_i	Generator bid price at bus i
$PD_i,\ QD_i$	Real and reactive power consumed at bus i
$Y_{ij}\angle\theta_{ij}$	Bus admittance matrix element between buses i and j
$y_{ij}\angle\phi_{ij}$	Line admittance element between buses i and j
$\underline{V_i},\ \overline{V_i}$	Minimum and maximum voltage limits at bus i
$\overline{SL_k}$	Maximum apparent power flow possible in line k
NT	Total number of transmission lines and transformers
$\underline{PG_i},\ \overline{PG_i}$	Minimum and maximum real power generation limits at bus i
$\underline{QG_i},\ \overline{QG_i}$	Minimum and maximum reactive power generation limits at bus i
$\overline{PR_i}$	Maximum demand response limit at bus i
b	Constants in generator's price offer curve
L, M, N	Number of neurons in neural network Layers 3, 2, and 1 respectively
XO_n	Normalizing offset for neuron n in Layer 1
XG_n	Normalizing gain for neuron n in Layer 1
XM	Normalizing minimum in Layer 1
$b1_m$	Offset for neuron m in Layer 2
$IW1_{nm}$	Weight for neurons m and n in Layer 2
$b2_l$	Offset for neuron l in Layer 3
$LW2_{ml}$	Weight for neurons m and l in Layer 3
YM_l	Normalizing minimum for neuron l in Layer 4
YG_l	Normalizing gain for neuron l in Layer 4
YO_l	Normalizing offset for neuron l in Layer 4

C. Variables

$PG_i,\ QG_i$	Real and reactive power generated at bus i
PR_i	Total demand response dispatched at bus i
$V_i\angle\delta_i$	Voltage phasor at bus i
$SF_k,\ ST_k$	Apparent power flow from and to line k respectively
λ_i	Locational marginal price at bus i
XP_n	Output from neuron n in Layer 1
$a1_m$	Output from neuron m in Layer 2
$a2_l$	Output from neuron l in Layer 3

Manuscript received February 19, 2020; revised July 5, 2020; accepted August 15, 2020. Date of publication September 1, 2020; date of current version February 19, 2021. This work was supported by the Financial support from NSERC is gratefully acknowledged. Paper no. TPWRS-00267-2020. *(Corresponding author: Bala Venkatesh.)*

The authors are with the Department of Electrical, Computer, and Biomedical Engineering and the Centre for Urban Energy at Ryerson University, Toronto, ON M5B2K3, Canada (e-mail: jessie.ma@ryerson.ca; bala@ryerson.ca).

Color versions of one or more of the figures in this article are available online at https://ieeexplore.ieee.org.

Digital Object Identifier 10.1109/TPWRS.2020.3020856

I. INTRODUCTION

WITH the increased adoption of smart technologies, flexible resources such as Demand Response (DR) have more opportunities in electricity markets to help deliver greater value to consumers. This, however, requires that electricity market operators and regulators both allow for the economic benefits of DR while shielding consumers from any harmful effects.

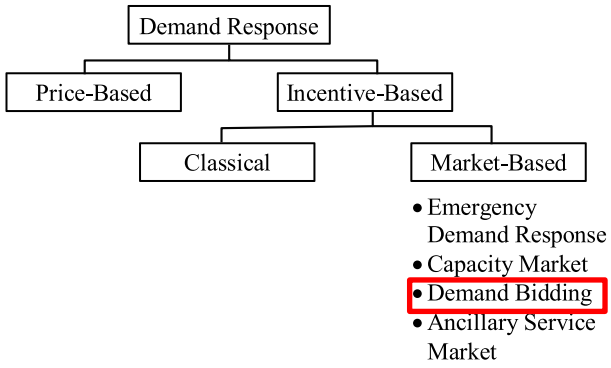

Fig. 1. Demand response categories and sub-categories.

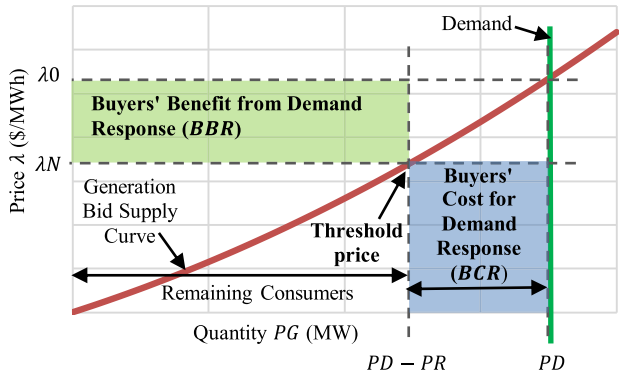

Fig. 2. Electricity market settlement graph showing threshold price from FERC Order 745's Net Benefits Test.

A. Demand Response Categories

DR is "changes in electric usage by demand-side resources from their normal consumption patterns in response to changes in the price of electricity over time, or to incentive payments designed to induce lower electricity use at times of high wholesale market prices or when system reliability is jeopardized." [1] This is a broad definition that encompasses a wide variety of DR types, as shown in Fig. 1. At the most basic level, DR can be classified as *price-based* or *incentive-based*. [2]–[5] *Price-based DR* changes its consumption level in response to changes in price, whereas *incentive-based DR* responds to a financial incentive. Within the incentive-based category, there are market-driven programs and classical programs. Deeper in the market-driven programs are those that pay for capacity and those that pay for energy through demand bidding, among others.

This paper focuses on the market-driven incentive-based DR programs in which DR is compensated for their services through demand bidding.

B. Federal Energy Regulatory Commission's Order 745

In 2011, the Federal Energy Regulatory Commission (FERC) in the United States issued Order 745 [6]. This Order stipulates two main policies: (a) that Independent System Operators (ISOs) and Regional Transmission Organizations (RTOs) procure DR if it passes a Net Benefits Test (NBT); and (b) that DR is paid at the Locational Marginal Price (LMP). In this paper, we present an optimal power flow (OPF) formulation that implements both parts of Order 745.

The first part of Order 745 requires the NBT, which compares the incremental benefits and costs associated with purchasing DR. If the benefits exceed the costs, the NBT is passed, and the DR purchase is permitted. If the costs exceed the benefits, DR is not purchased. The NBT is intended to protect consumers by limiting DR purchase to a quantity that is economically advantageous to consumers.

The second part of Order 745 requires DR to be paid at LMP. This is a policy decision made by FERC. We adopt this policy in the formulation proposed in this paper and demonstrate it with examples.

While FERC does not prescribe how ISOs and RTOs implement the NBT in Order 745, ISOs and RTOs must submit their plans to FERC for approval. These plans are discussed in the following section.

C. Implementation of Order 745 in Practice

ISOs and RTOs typically implement both parts of Order 745 in two stages. The first stage is a monthly determination of a threshold price (or corresponding quantity) beyond which DR cannot be procured. The second stage uses that threshold price (or corresponding quantity) in the day-ahead and real-time electricity markets [7], [8].

In the first stage, a generator supply bid curve is created for the upcoming month using actual historic bids, adjusted with forecasted fuel prices and resource availability. The point at which the incremental *benefits* from DR equal the incremental *costs* of DR defines the *threshold price*.

In the illustrative electricity market settlement graph in Fig. 2, the threshold price is marked. Whenever the LMP is higher than the threshold price, DR can be purchased and paid at LMP because the NBT is passed. This threshold price is posted online before the start of every month and is static throughout that month (e.g. [9]–[11]). When LMP is lower than the threshold price, DR is not permitted to be purchased due to failure of the NBT.

DR affects the electricity market in a unique way. The procurement of DR reduces the amount of total generation required and thereby displaces the most expensive generation units. In Fig. 2, with DR, the total quantity of generation dispatched moves from PD to $PD - PR$, while the price paid to that generation moves from $\lambda 0$ to λN. This results in new additional surplus for consumers, shown as the buyers' benefit from DR (BBR). Meanwhile, consumers incur new additional costs to buy the DR, shown as the buyers' cost for DR (BCR).

Mathematically, as seen in Fig. 2, for changes in price ($\lambda 0 - \lambda N$) and corresponding changes in quantity (PR), BBR and BCR are:

$$BBR = (\lambda 0 - \lambda N) \cdot (PD - PR) \tag{1}$$

$$BCR = PR \cdot \lambda N \tag{2}$$

where $\lambda 0$ is a function of PD equaling $\lambda(PD)$ and λN is a function of PD and PR equaling $\lambda(PD - PR)$.

Net Benefit is defined using (1) to (2) as below:

$$Net\ Benefit = BBR - BCR$$

$$Net\ Benefit = (\lambda 0 - \lambda N) \cdot PG - PR \cdot \lambda N \tag{3}$$

Using (3), the net benefit per unit of electricity enjoyed by paying consumers $(PD - PR)$ equals:

$$\frac{Net\ Benefit}{PD - PR} = \frac{BBR - BCR}{PD - PR} = \lambda(PD) - \frac{\lambda\,(PD - PR) \cdot PD}{PD - PR} \tag{4}$$

The maximum net benefits can be found by setting the partial derivative of (4) with respect to $PD - PR$ to zero:

$$\frac{\partial\left(\frac{Net\ Benefits}{PD-PR}\right)}{\partial\,(PD - PR)} = -\left[\frac{\frac{\partial\lambda(PD-PR)}{\partial(PD-PR)} \cdot PD \cdot (PD-PR) - \lambda\,(PD-PR) \cdot PD}{(PD-PR)^2}\right] = 0 \tag{5}$$

Simplifying right hand side of (5), we obtain the equality below that maximizes the net benefit per unit of electricity consumed, thereby mathematically defining the threshold price:

$$\left[\frac{\partial\,\lambda\,(PD - PR)}{\partial\ (PD - PR)}\right] \cdot \frac{PD - PR}{\lambda\,(PD - PR)} = 1 \tag{6}$$

In the second stage, the day-ahead and real-time electricity markets are settled. At any time period in which the LMP is greater than the threshold price in (6), ISOs and RTOs are permitted to purchase DR. DR vendors are paid at the prevailing LMP and settled out-of-market.

D. Shortcomings of Implementation of Order 745 in Practice

A main shortcoming of this approach is the monthly approximation of the generation supply bid curve will not be accurate for every time period of every day. These differentials will lead to either over- or under-purchasing of DR and sub-optimal prices for consumers. This problem has been recognized in the consultations FERC conducted for Order 745, and FERC ruled that the simplification of using monthly threshold prices was an acceptable compromise due to the complexities of implementing a single-stage method and the gap in knowledge then [6]. We address this shortcoming by integrating the NBT into a single-stage formulation in which we use the actual generator supply bid curve for that time period.

Another issue with the implementation of FERC Order 745 in practice is the system-wide application of NBT. This does not consider line limits and congestion, so it is possible for DR to be dispatched in one zone and when it is actually needed in another zone. Furthermore, the generation supply curve used in this process will not capture LMP variations caused by local line congestions. Hence, local DR requirements due to higher LMPs at certain busses could differ than the system-wide conditions, leading to sub-optimal DR procurement.

E. Implementation of Order 745 and Demand Response in Academic Literature

There are a very few academic works on the implementation of FERC's NBT. One study adopts the NBT implementation used in practice (as detailed in the previous section) and then proposes a new method to enhance the NBT by exploiting the differences between wholesale and retail prices [12]. A second study aims to minimize utilities' financial losses due to the difference between wholesale and retail prices during abnormal events by iterating through different DR incentive prices [13]. It considers the net benefits of DR. To our knowledge, there are no additional examples of NBT implementations in literature.

More generally, published literature shows the implementation of DR formulations in the absence of NBT. A common objective is the minimize total costs, including the costs paid to DR service providers [14]–[18]. This approach treats DR identically to generation. It also assumes a single-ended auction, in which minimizing total costs of a single commodity equates maximizing social welfare. (Social welfare "is defined as the summation of consumer surplus and supplier surplus," [19] and it represents the collective benefit for all market participants in society.) However, two commodities are being procured simultaneously – generation and DR – and the purchase of DR decreases the pool of paying customers. Therefore, simply minimizing total costs while leaving DR unconstrained no longer maximizes social welfare. One other paper overtly maximizes social welfare, but does not account for the change in demand due to DR [20]. None of these studies place a limit on the quantity of DR that is permitted to be procured, as FERC's NBT does.

F. Motivation for and Contributions of This Work

FERC's ruling points to the need for academic exploration to create more efficient and effective methods of implementing the NBT. Our work responds to this call.

In this paper, we propose a mechanism to optimize electricity market (real-time or near real-time) with bus-wise NBT. This is more accurate and efficient than the current practice of a monthly, system-wide NBT implementation.

The main contributions of this work include:

a) *Single-stage real-time or near real-time OPF with NBT* – Rather than the monthly approximations of the generator supply curve used today in the two-stage implementation, our method is implemented in a single stage, with the NBT directly integrated into the OPF formulation. This results in greater accuracy as the real-time supply curves and load levels at each bus are considered.

b) *Bus-wise NBT implementation considering full transmission network* – Because we apply the NBT at the bus-level, the entire transmission network including congestion, line limits, reactive power limits, and voltage limits are modeled and recognized. These considerations are absent in existing system-wide NBT implementations, leading to sub-optimal outcomes.

G. Organization of the Paper

This paper is organized as follows. Background information, including DR categories, FERC Order 745, and an academic literature review, is in Section I. The proposed OPF including the new NBT constraint is presented in Section II. Results of the case studies are in Section III. Practical considerations are discussed in Section IV. Conclusions are in Section V. Lastly, the Appendix contains the theory and procedure for training the neural networks used in the case studies in this paper.

II. Proposed Optimal Power Flow Formulation With Net Benefits Test for Demand Response

The objective is to maximize social welfare by minimizing total costs for a single-ended auction:

$$Minimize\ Total\ Costs\ = \sum_{i=1}^{NB}\sum_{q=0}^{NQ} b_{i,q}\cdot PG_i{}^q \qquad (7)$$

The optimization problem is subject to the following constraints:

a) Real power balance

$$PG_i + PR_i - PD_i - V_i\sum_{j=1}^{NB} V_j\cdot Y_{ij}\cdot\cos\langle\delta_i{-}\delta_j{-}\theta_{ij}\rangle = 0,\ \forall i = 1\ to\ NB \qquad (8)$$

b) Reactive power balance

$$QG_i - QD_i - V_i\sum_{j=1}^{NB} V_j\cdot Y_{ij}\cdot\sin\langle\delta_i-\delta_j-\theta_{ij}\rangle = 0,\ \forall\, i = 1\ to\ NB \qquad (9)$$

c) Voltage limits

$$\underline{V_i} \le V_i \le \overline{V_i}\ \forall\ i\ =\ 1\ \text{to}\ NB \qquad (10)$$

d) Line flow limits

$$SF_k = [(V_i\angle\delta_i - V_j\angle\delta_j)\cdot y_{ij}\angle\phi_{ij}]^*\ \cdot V_i\angle\delta_i\forall\ k\ =\ 1\ \text{to}\ NT,\ \{i,j\}\in k \qquad (11)$$

$$ST_k = [(V_j\angle\delta_j - V_i\angle\delta_i)\cdot y_{ij}\angle\phi_{ij}]^*\ \cdot V_j\angle\delta_j\forall\ k\ =\ 1\ \text{to}\ NT,\ \{i,j\}\in k \qquad (12)$$

$$|SF_k| \le \overline{SL_k}\ \forall\ =\ 1\ \text{to}\ NT;\forall\ k\ =\ 1\ \text{to}\ NT \qquad (13)$$

$$|ST_k| \le \overline{SL_k}\ \forall\ =\ 1\ \text{to}\ NT;\forall\ k\ =\ 1\ \text{to}\ NT \qquad (14)$$

e) Generator real and reactive power limits

$$\underline{PG_i} \le PG_i \le \overline{PG_i}\ \forall\ i\ =\ 1\ \text{to}\ NB \qquad (15)$$

$$\underline{QG_i} \le QG_i \le \overline{QG_i}\ \forall\ i\ =\ 1\ \text{to}\ NB \qquad (16)$$

f) New Constraint for DR

From (6), net benefit is maximized at a bus that offers DR when it is subject to:

$$\left[\frac{\partial\lambda_i}{\partial\left(PD_i - PR_i\right)}\right]\cdot\frac{PD_i - PR_i}{\lambda_i} \ge 1\ \forall\ i\ =\ 1\ \text{to}\ NB \qquad (17)$$

The equality in (6) is turned into a 'greater than or equal to' constraint to enable feasible solutions when $\overline{PR_i}$ is less than that available to get an optimal solution.

The formulation is indifferent to the form of the supply curve λ. Our method is versatile and can apply to continuously differentiable supply curves of any form.

In order to implement (17), both the supply curve λ_i and its partial derivative $\frac{\partial\lambda_i}{\partial(PD_i-PR_i)}$ must be known in advance for every bus i that offers DR. The proposed method considers modelling this relationship by repeatedly solving OPF for various values of demand response at every bus with DR. This dataset captures the non-linear relationship between price λ_i and DR. It is used to train a neural network and is used in (17) through equations described in (20)–(29), which are presented in the Appendix. Detailed steps for our methodology using neural networks are in the Appendix.

g) DR limits at every bus that offers DR

$$0 \le PR_i \le \overline{PR_i}\ \forall\ i\ =\ 1\ \text{to}\ NB \qquad (18)$$

Constraint (18) ensures that DR is within the limits of what can be offered due to equipment or other restrictions.

Classic nonlinear optimization techniques can solve this nonlinear optimization problem completely described in (7)–(18).

III. Results & Discussion

Our proposed method was applied to a sample 4-bus system, a modified version of the IEEE-118-bus test system, and the Transmission system in Ontario, Canada. We show the optimal quantity of DR to be dispatched at every bus and the resulting impacts of DR procurement on performance. For all the case studies, we compare three scenarios:

(S1) OPF results without DR (i.e. $\overline{PR_i} = 0,\ \forall\ i\ =\ 1\ to\ NB$) obtained using the NBT formulation (7)–(18) proposed in this paper;
(S2) OPF results obtained using the NBT formulation (7)–(18) proposed in this paper; and
(S3) OPF results by solving (7)–(16) and (18), similar to existing OPF methods with DR (i.e. without NBT) [14]–[18].

We will show that our formulation (7)–(18) with NBT (S2) will maximize net benefits and will perform better than the other scenarios (S1) and (S3) for all consumers.

Neural network-based models were used for these case studies to implement the NBT constraint (17), and the detailed procedure to create these neural network models is described in the Appendix. However, users are free to choose any method that best suits their systems to model the relationships between LMP λ at every bus and the net load PD at all the buses, as long as λ is continuously differentiable.

A. 4-Bus Test System

The 4-bus test system has two generation buses and two load buses, as shown in Fig. 3. DR was limited at buses 4 and 3 such that $\overline{PR_4}$ is 0 MW and $\overline{PR_3}$ is 300 MW.

Both generators are 1,000 MW each and have supply costs of the form (7) with the coefficients listed in Table I. Line limits

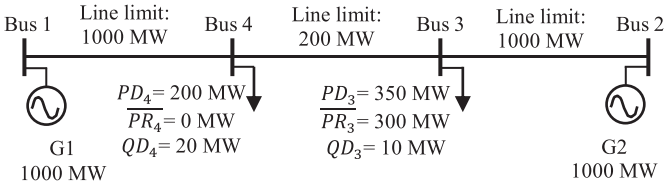

Fig. 3. 4-bus test system.

TABLE I
GENERATOR COEFFICIENTS FOR 4-BUS TEST CASE

Bus	b_0 ($)	b_1 ($/MW)	b_2 ($/MW^2)	b_3 ($/MW^3)	b_4 ($/MW^4)
1	100	5	0.1	0	0
2	500	50	0.1	0.01	0.00001

TABLE II
RESULTS FOR 4-BUS SYSTEM WITHOUT DEMAND RESPONSE (S1)

Bus	*PG* (MW)	*PD* (MW)	*PR* (MW)	λ ($/MW)
1	401.1	0	0	85.21
2	150.4	0	0	894.98
3	0.0	350	0	896.77
4	0.0	200	0	85.67

TABLE III
RESULTS FOR 4-BUS SYSTEM WITH PROPOSED NET BENEFITS TEST FORMULATION (S2)

Bus	*PG* (MW)	*PD* (MW)	*PR* (MW)	λ ($/MW)
1	401.05	0	0	85.21
2	31.08	0	0	86.40
3	0	350	119.21	86.44
4	0	200	0	85.66

TABLE IV
RESULTS FOR 4-BUS SYSTEM WITH DEMAND RESPONSE AND WITHOUT NET BENEFITS TEST (PUBLISHED METHODS) (S3)

Bus	*PG* (MW)	*PD* (MW)	*PR* (MW)	λ ($/MW)
1	242.3	0	0	53.45
2	8.2	0	0	53.65
3	0.0	350	300	53.65
4	0.0	200	0	53.62

between buses 1 and 4 and between buses 2 and 3 are 1000 MW, with a tighter limit of 200 MW between buses 3 and 4, as shown in Fig. 3.

By performing five OPFs (7)–(16) and (18), one for each of the five different DR levels, training data for neural network was generated. These five cases were then used for training, testing, and validating the neural network thus generating neural network parameters for the 4-bus system. Details are in the Appendix.

Thereafter, the 4-bus system was evaluated for three scenarios: (S1)–(S3).

The results in the absence of DR (S1) are shown in Table II. Results for our proposed formulation (S2) are shown in Table III with an optimal DR quantity (PR) of 119.21 MW at bus 3. For comparison, the results for the same system using existing published methods (S3) [14]–[18] (i.e. with DR but without the NBT constraint) are in Table IV.

TABLE V
COMPARISON OF PERFORMANCE RESULTS AT BUS 3 FOR 4-BUS TEST CASE

Scenario	Actual Price ($/MW)	Benefit due to DR (BBR) ($)	Cost of DR (BCR) ($)	Net Benefit due to DR ($)
S1. No DR	896.77	-	-	-
S2. NBT	**131.09**	187,017.76	10,304.22	**176,713.54**
S3. DR only Ref. [14]–[18]	**375.56**	42,156.14	16,095.60	**26,060.54**

Table V shows a comparison of key performance metrics of the three scenarios at bus 3. The net benefit defined in (3) was calculated to show that it is being maximized and the NBT is indeed being respected.

In order to capture the economic effect of NBT on customers, we compute Actual Prices at bus 3. Actual Prices reflect total payments which equals sum of: (a) payments based upon LMPs to generators for energy; and (b) payments based upon LMPs to DR units for service [21], [22]. This concept has been used in industry as well. While the term Actual Price had not been coined yet at the time, the Southwest Power Pool measured the impact to consumers using Actual Price [23]. FERC's Order 745 also describes the billing unit effect due to the reduced pool of paying consumers [6], and this is captured by Actual Price. Given that DR units reduce demand and accordingly do not pay for receiving energy, Actual Price at a bus is defined as below:

$$Actual\ Price\ at\ bus\ i\ = \frac{\lambda_i\,(PD_i - PR_i)\cdot PD_i}{PD_i - PR_i} \tag{19}$$

Examining (4), it can be seen that Actual Price is the second term on the right side of the equation. The difference between LMP without DR and Actual Price with DR equals the Net Benefit per unit of electricity consumed.

Clearly, our proposed formulation integrating DR (S2) performed the best of the three scenarios, yielding the maximum net benefits to the market and the lowest Actual Prices for remaining consumers. With our proposed method (S2), the net benefits for consumers at bus 3 are maximized at $176,713.54, which is 578% more than their net benefits of $26,060.54 from existing published methods (S3). Furthermore, consumers at bus 3 can pay a lower Actual Price of $131.09 in S2 than $375.56 in S3. This represents a savings of 65.1%.

This example demonstrates that, while DR service might lower LMP, it is important to limit its procurement to that value where NBT is maximized.

To verify and validate the quality of the results, the Actual Price was examined for the full range of available DR quantities to ensure that S2, with the NBT constraint, does indeed produce the optimal result. Fig. 4 shows the Actual Price as the quantity of DR changes. Clearly, the optimal DR quantity of 119.21 MW from S2 aligns with the minimum Actual Price in this region, and this validates the superior performance of the NBT constraint in S2.

B. 118-Bus Test System

To demonstrate that our proposed method (7)–(18) works on a larger practical power system, it was tested on a modified IEEE

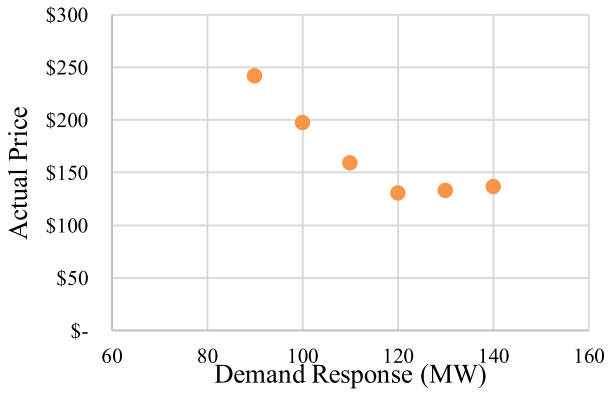

Fig. 4. Actual Price on the 4-bus study case.

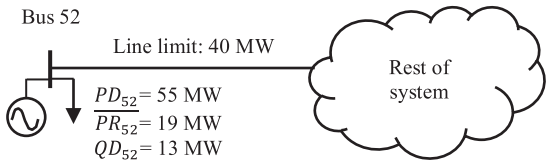

Fig. 5. 118-bus test case 1.

TABLE VI
GENERATOR COEFFICIENTS FOR 118-BUS TEST CASE 1

Bus	b_0 ($)	b_1 ($/MW)	b_2 ($/MW^2)	b_3 ($/MW^3)	b_4 ($/MW^4)
52	500	50	0.1	0.01	0.00001
All others	100	5	0.1	0	0

118-bus system. A real-life system could be reduced to a series of internally-uncongested zones as buses for this analysis. For instance, the IESO in Ontario, Canada, plans and operates its system based on ten transmission zones [24]. Therefore, testing our proposed method on a 118-bus system – which has more buses than some real-life systems have zones – demonstrates its practical application.

We considered two cases in which DR can be useful: (a) line congestion restricts access to inexpensive generation; and (b) exhausted limits of inexpensive generation. In both cases, consumers would be forced to resort to expensive generation in the absence of DR.

1) Case 1: Line Congestion: In this case study, bus 52, a terminal bus with expensive generation and 55 MW in load, is connected to the rest of the system through a restricted line with a line flow limit of 40 MW. All other lines are uncongested. Generator price coefficients of the form (7) are in Table VI. DR is offered only on bus 52.

Again, a neural network was created using the procedure in the Appendix. The load on bus 52 was adjusted to 21 different levels, and an OPF was performed for each. The results from those 21 cases were used to train the neural network and, in turn, used in the NBT constraint (17) in the main formulation.

As before, three scenarios were evaluated: (S1)–(S3).

TABLE VII
RESULTS FOR 118-BUS TEST CASE 1

Scenario	PR (MW)	λ ($/MW)	Actual Price ($/MW)	Benefit due to DR (BBR) ($)	Cost of DR (BCR) ($)	Net Benefit due to DR ($)
Bus 52: PD = 55 MW						
S1. No DR	0.0	60.41	60.41	-	-	-
S2. DR & NBT	16.92	20.01	**28.90**	1,538.49	338.63	**1,199.86**
S3. DR only Ref. [14]–[18]	19	20.00	**30.55**	1,455.00	379.97	**1,075.03**

TABLE VIII
GENERATOR COEFFICIENTS FOR 118-BUS TEST CASE 2

Bus	b_0 ($)	b_1 ($/MW)	b_2 ($/MW^2)	b_3 ($/MW^3)	b_4 ($/MW^4)
Expensive	0	500	10^{-8}	0	0
Inexpensive	50	50	10^{-6}	0	0

The results at bus 52 for the three scenarios are shown in Table VII. Our NBT constraint (17) has limited the DR procurement to 16.92 MW in S2, whereas the equipment limit of 19 MW was procured in S3 under existing DR procurement methods.

Our proposed NBT formulation has led to optimal net benefits of $1,199.86 in S2, whereas existing methods would produce 1.6% lower net benefits of $1,075.03. Actual Price is also lower at $28.90 in S2, compared to $30.55 in S3 – a savings of 5.4%.

This example clearly demonstrates the proposed method can be applied to implement NBT when the network limitations require procurement of DR. The results show that by using the proposed method DR procurement is limited to a quantity that both satisfies and optimizes NBT.

2) Case 2: Limited Inexpensive Generation: The second 118-bus case study considers a system in which approximately 95% of the total load is supplied with inexpensive generation at maximum output capacity, and the remaining 5% comes from much more expensive sources. DR has the potential to avoid dispatching the expensive generation units. The generator price coefficients of the form (7) are in Table VIII. There were 10 inexpensive generator units scattered across the system, totaling 3,800 MW. Total system load is 3,799 MW. All lines are uncongested. DR is offered on four buses: 22, 25, 36, and 117.

A neural network was fitted to this system with four DR levels at each of the four buses with DR according to the procedure in the Appendix. These 256 OPF results were used to train, test, and validate the neural network, which then informs the NBT constraint (17) in the main formulation.

Fig. 6 shows the average LMP across all 118 buses versus the total system load for the 256 scenarios used as inputs into the neural network. Clearly, there is a sharp increase in average price when system load increases after the inexpensive generation units are used up.

The same three scenarios were evaluated: (S1)–(S3). The results for the four buses offering DR are in Table IX.

The results clearly show that at each bus offering DR, the net benefits are greater when using our proposed NBT formulation (S2) rather than existing published methods for DR procurement

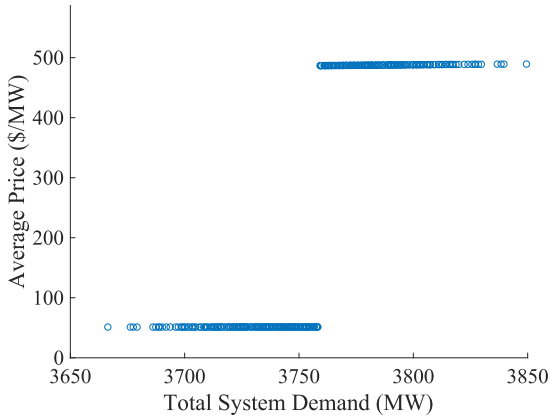

Fig. 6. Average price vs. total system demand for 256 neural network input scenarios for 118-bus test case 2.

TABLE IX
RESULTS FOR 118-BUS TEST CASE 2

Scenario	PR (MW)	λ ($/MW)	Actual Price ($/MW)	Benefit due to DR (BBR) ($)	Cost of DR (BCR) ($)	Net Benefit due to DR ($)
Bus 22: PD = 109.7 MW						
S1. No DR	0.0	492.07	492.07	-	-	-
S2. DR & NBT	24.6	51.58	**66.47**	37,510.87	1,268.30	**36,242.58**
S3. DR only Ref. [14]–[18]	44.5	51.33	**86.31**	28,767.01	2,283.16	**26,483.85**
Bus 25: PD = 269.0 MW						
S1. No DR	0.0	491.40	491.40	-	-	-
S2. DR & NBT	37.5	51.51	**59.85**	101,855.98	1,930.39	**99,925.58**
S3. DR only Ref. [14]–[18]	109.0	51.27	**86.21**	70,419.90	5,589.72	**64,830.19**
Bus 36: PD = 126.3 MW						
S1. No DR	0.0	492.53	492.53	-	-	-
S2. DR & NBT	18.1	51.61	**60.27**	47,670.15	936.32	**46,733.83**
S3. DR only Ref. [14]–[18]	51.2	51.43	**86.48**	33,121.51	2,631.75	**30,489.76**
Bus 117: PD = 97.3 MW						
S1. No DR	0.0	479.77	479.77	-	-	-
S2. DR & NBT	2.6	50.29	**51.67**	40,694.69	130.31	**40,564.38**
S3. DR only Ref. [14]–[18]	39.5	50.16	**84.35**	24,871.65	1,978.98	**22,892.68**

(S3). In fact, S2 produced net benefits of 36.8%, 54.1%, 53.3%, and 77.2% higher than S3 at each of the four buses offering DR. Also, S2 yielded Actual Prices lower by 23.0%, 30. 6%, 30.3% and 38.7% at those buses when compared to S3. The NBT constraint resulted in less DR procured in S2 than in S3 for every bus, however, buying less DR resulted in better performance in terms of greater net benefits and lower Actual Prices for consumers.

This second case for the 118-bus system demonstrates the value of the NBT in a large, uncongested system in which inexpensive generation resources have been exhausted. DR has the capability to avoid buying from expensive generation suppliers (S1). Furthermore, the NBT constraint (S2) can avoid over-purchasing DR (S3) and going beyond the optimal point for both Actual Price and net benefits.

TABLE X
RESULTS FOR ONTARIO CASE

Scenario	PR (MW)	λ ($/MW)	Actual Price ($/MW)	Benefit due to DR (BBR) ($)	Cost of DR (BCR) ($)	Net Benefit due to DR ($)
Niagara Zone, Bus 7: PD = 3,600 MW						
S1. No DR	-	4,734	4,734	-	-	-
S2. DR & NBT	288	931	**1,042**	9,171,719	268,304	**8,903,415**
S3. DR only Ref. [14]–[18]	500	866	**1,063**	8,508,825	433,032	**8,075,793**

C. Ontario, Canada

To further validate the practicality of our proposed method, we tested it on a system based on Ontario, Canada. The IESO, the system operator in Ontario, models the province's Transmission system as ten internal zones, which are shown in Fig. 7. Each zone was assigned a bus number, which are indicated in the blue circles. Both the Northwest and Niagara zones were split and assigned two bus numbers each: one for generation and one for load. Thirteen lines connect the 12 buses, and the lines are indicated in the white circles. System data was gathered from publicly available information where possible. Historical data from the IESO was used for the zonal loads [25], installed generator capacities [26], and interzonal line ratings [24]. Since generator bid data is not available in Ontario, the actual bids from PJM were used instead. [27] The units were randomly allocated to Ontario's zones so that the installed generator capacity in each zone was covered. Those units were then stacked and fitted with a polynomial curve. Demand response availability was assigned to the Niagara Zone's load bus, Bus 12.

A neural network was produced for this system using the OPFs from 10 loading levels in the Niagara Zone according to the procedure detailed in the Appendix. Additional points were created via interpolation to facilitate the neural network training, resulting in 900 input data points. The results of the neural network were then fed into the NBT constraint (17) in the main formulation. The three scenarios, S1–S3, were evaluated again, and the results are shown in Table X.

Again, the results demonstrate the superior performance of S2, DR with NBT, over S1 and S3. Our NBT method (S2) produces a net benefit of $8,903,415.44 – an improvement of 10.2% over the existing methods (S3), which yields a net benefit of $8,075,793.15. The Actual Price is improved by 2.0% – from $1,062.90 to $1,042.01 – when the NBT constraint in our method (S2) is used instead of existing methods found in literature (S3) [14]–[18].

IV. PRACTICAL CONSIDERATIONS

There are several practical aspects to be considered in the training, adaptation and implementation of the neural networks.

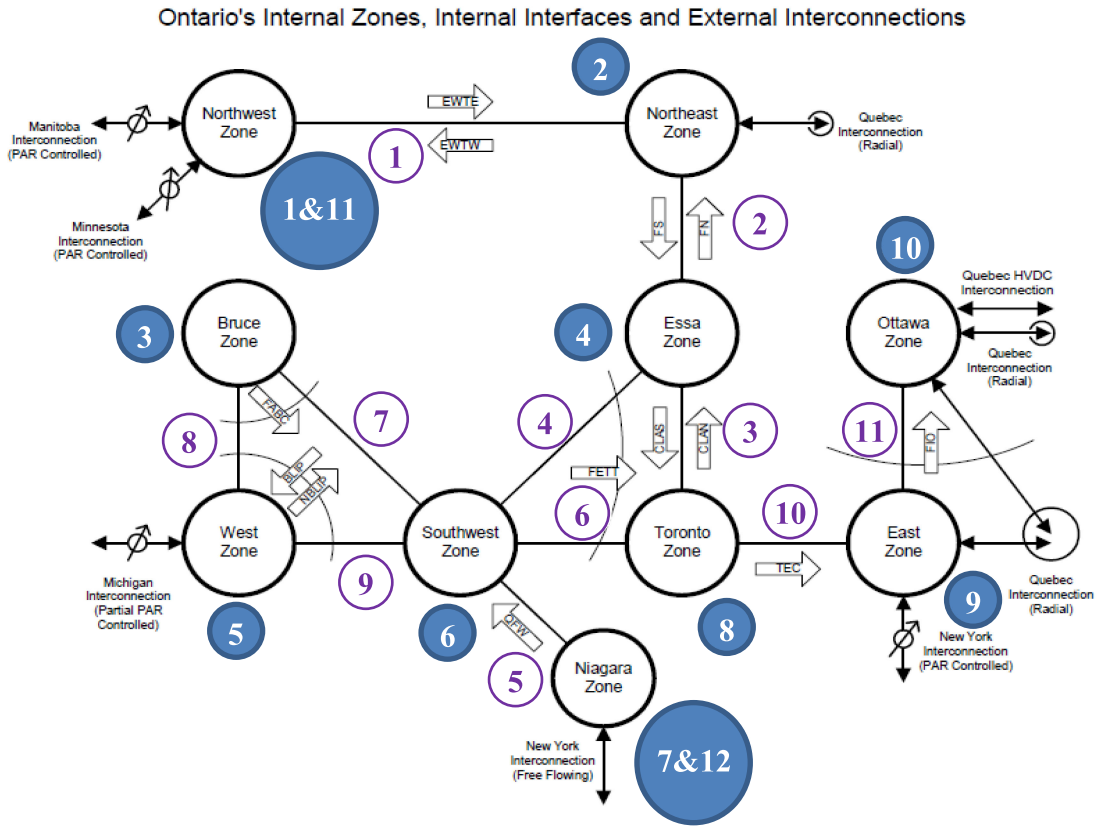

Fig. 7. Ontario's ten Transmission zones [24].

A. Adapting the Neural Network Continually

While the choice to use neural networks or another method rests with the user, neural networks were found to be well suited for the case studies reported in this paper. Neural networks are robust for mapping multi-variate complex spaces. Once a neural network is trained, with the evolution of time, additional input/output combinations may arise that are not mapped yet. Accordingly, a trained neural network can be updated to include these new input/output combinations. The neural network training process is incremental, and new information and data can be used to update its weights. For example, MATLAB has a built-in function in the Deep Learning Toolbox to update weights and biases of a trained neural network with new data points [28].

B. Interpolation

The relationship between input (loading levels) and output (LMP values) is assumed to be linearly varying. Accordingly, via interpolation, additional input/output combinations are created. This leads to additional training points for the neural network, making it robust and accurate. It also contains the time required to generate input/output combinations via OPF. Further, with the evolution of time, additional input/output combinations that become available can be used to update the neural network using the process outlined in the preceding section.

The Ontario case had 10 loading levels. However, only 10 loading levels were insufficient to produce a robust neural network. Therefore, additional data points were created by interpolating while limiting processing time increases associated with additional OPF runs. This yielded a total of 900 data points as input to train the neural network. This method also addresses concerns about the minimum number of loading levels required for the neural network and sensitivities to modelling inaccuracies.

V. Conclusion

In the decade since FERC Order 745 was issued, the gap in academic literature on real-time or near real-time implementations of the NBT for DR still persists. Existing NBT implementations in practice involve a monthly calculation of a system-wide threshold quantity of permitted DR based on monthly approximations of generator price bids and total system demand. Without our NBT formulation, consumers would be foregoing net benefits while being exposed to higher Actual Prices.

We propose a new OPF formulation with a new constraint for the NBT to ensure the quantity of DR at each bus respects the threshold and net benefit is maximized, thereby ensuring that the benefits of DR outweigh the costs and that consumers are protected.

Our method offers two key advantages: (a) a real-time or near real-time approach captures the time-based nuances that a monthly NBT test disregards for both generation pricing and

demand changes; and (b) a bus-wise implementation that considers congestion, line limits and network model, thereby yielding a feasible and more accurate solution.

The new method was tested on a 4-bus test system, a 118-bus modified IEEE test system, and the Transmission system in Ontario, Canada, showing higher net benefits and lower Actual Prices than conventional DR dispatch methods. For the 4-bus case, consumers at the bus offering DR increased their net benefits by 578% and reduced their Actual Price by 65.1% when using our proposed method, as compared to methods existing in literature. For the first 118-bus case, DR provided congestion relief, and our method increased net benefits by 1.6% and reduced Actual Price by 5.4% when compared to conventional DR procurement methods. The second 118-bus case was a system with limited inexpensive generation. Consumers at the four buses offering DR increased their net benefits by 36.8% to 77.2% and reduced their Actual Prices by 23.0% to 38.7% when compared to existing DR procurement methods. The Ontario case showed an increase in net benefits of 10.2% and a decrease in Actual Price of 2.0%.

Furthermore, these test cases showcase scenarios in which DR and the NBT are particularly useful: for congestion relief and for displacing the dispatch of expensive generation units.

While we trained neural networks to model the effects of DR levels on pricing at each bus in our test cases, users are free to choose any mathematical model for their systems, so long as the model is continuously differentiable in the region of interest (i.e. for the amounts of DR under consideration).

For next steps, it would be useful to test this method in trial runs in real-time or near-real-time optimizations. While we have tested this offline for the Ontario system, there could be additional unforeseen complexities associated with implementation, particularly around adapting existing software systems.

There is growing potential for DR as the costs of smart technologies drop, aging grids with limited room for expansion need to be used more efficiently, and consumption patterns evolve due to EVs and intermittent distributed renewables. The NBT implementation proposed in this paper shows how DR to be integrated to the mutual advantage of both consumers and DR providers.

APPENDIX
NEURAL NETWORKS TRAINING

At every bus that offers DR, the NBT asserts that there is a threshold point up to which DR can be purchased and net benefits will surpass net costs. A differentiable equation is needed for the supply price curve λ at every bus due to locational pricing. Furthermore, λ is dependent on the loading levels on all the buses. Due to these complexities, neural networks were used in the test cases in this paper to: (i) determine an accurate mathematical relationship between λ and all the variables at every bus; and (ii) by differentiating λ, the threshold point to be implemented in the NBT constraint (17). Furthermore, only the section of the curve where DR is offered needs to be modelled.

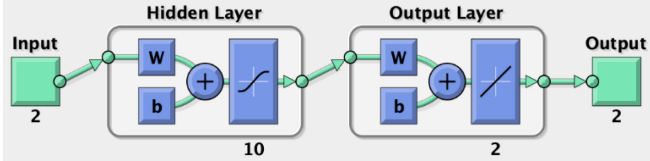

Fig. 8. Neural network map [29].

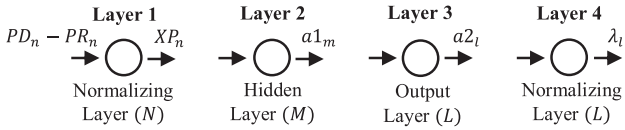

Fig. 9. Neural network layers.

The procedure used in the case studies is outlined next.

Step1: A number of loading scenarios were generated. In the 4-bus case study, five loading levels were considered at the load bus offering DR, so there were five scenarios. The first 118-bus case had 21 scenarios that varied the DR at one bus, while the second 118-bus case had four buses with four DR levels each, yielding 4^4, or 256, scenarios. The Ontario case had 10 loading levels, plus additional linearly interpolated points, for a total for 900 data points.

Step2: Optimal power flow was solved for each of the generated scenarios, yielding a locational marginal price at every bus. This forms the data set used for creating the neural network.

Step3: The relationship between LMP λ and the load levels at every bus for every scenario was determined using neural networks fitting. This relationship is continuously differentiable, so that it can be used in (17).

For the case studies, the Neural Net Fitting app in the Deep Learning Toolbox in MATLAB was used to solve a two-layer feed-forward problem, as shown in Fig. 8. The inputs were the net loading levels ($PD_i - PR_i$) at every bus i offering DR, and the outputs were the prices at every bus i offering DR. Seventy percent of the scenarios were used for training, 15% were used for validation, and 15% were used for testing. The Levenberg-Marquardt training algorithm was used, and there were 10 neurons in the hidden layer.

For clarity, one neuron from every layer can be represented as shown in Fig. 9. The first layer n has N nodes, and its purpose is to transform the inputs into a normalized range for further calculations. The second layer m is the hidden layer with M neurons and uses a sigmoid function. The third layer l is the output layer, uses a linear function, and has L neurons. Lastly, the fourth layer transforms the normalized outputs back to reality, and it also has L neurons. In our examples, N and L are both equal to the number of buses offering DR, and M is 10.

The relationship (20) between λ_l, the price at bus l, and $PD_{1..N} - PR_{1..N}$, the net loads at buses 1 to N, is a function of four sub- functions (21) to (24), one for each layer of the

neural network:

$$\lambda_l\left(PD_{1..N}-PR_{1..N}\right)=\lambda_l\ \left(a2_l\right)\cdot a2_l\left(a1_{1..M}\right)\cdot a1_{1..M}\left(XP_{1..N}\right)\cdot XP_{1..N}\left(PD_{1..N}-PR_{1..N}\right) \quad (20)$$

$$XP_n\ \left(PD_{1..N}-PR_{1..N}\right)=\left[\left(PD_{1..N}-PR_{1..N}\right)-XO_n\right]\cdot XG_n+XM \quad (21)$$

$$a1_m\left(XP_{1..N}\right)=\frac{2}{1+exp\left[-2\cdot\left(b1_m+\sum_{n=1}^{N}IW1_{nm}\cdot XP_n\right)\right]}-1 \quad (22)$$

$$a2_l\left(a1_{1..M}\right)=b2_l\ +\sum_{m=1}^{M}LW2_{ml}\cdot a1_m \quad (23)$$

$$\lambda_l\ \left(a2_l\right)=\frac{a2_l-YM_l}{YG_l}\ +YO_l \quad (24)$$

Step4: In order to implement the NBT constraint (17), the partial derivative of λ_l with respect to PD_n-PR_n (20), where l equals n because it is the same node or bus, is needed. This is found by using the chain rule to differentiate (20), yielding:

$$\frac{\partial\,\lambda_l}{\partial\ \left(PD_n-PR_n\right)}=\frac{\partial\,\lambda_l}{\partial\,a2_l}\cdot\sum_{m=1}^{M}\left(\frac{\partial\,a2_l}{\partial\,a1_m}\cdot\frac{\partial\,a1_m}{\partial\,XP_n}\right)\cdot\frac{\partial\,XP_n}{\partial\ \left(PD_n-PR_n\right)} \quad (25)$$

Differentiating each of the four components yields:

$$\frac{\partial\,XP_n}{\partial\ \left(PD_n-PR_n\right)}=XG_n \quad (26)$$

$$\frac{\partial\,a1_m}{\partial\,XP_n}=\frac{-2\cdot\left\{exp\left[-2\cdot\left(b1_m+\sum_{n=1}^{N}IW1_{nm}\cdot XP_n\right)\right]\right\}\cdot\left(-2\cdot IW1_{nm}\right)}{\left\{1+exp\left[-2\cdot\left(b1_m+\sum_{n=1}^{N}IW1_{nm}\cdot XP_n\right)\right]\right\}^2} \quad (27)$$

$$\frac{\partial\,a2_l}{\partial\,a1_m}=LW2_{ml} \quad (28)$$

$$\frac{\partial\,\lambda_l}{\partial\,a2_l}=\frac{1}{YG_l} \quad (29)$$

Step5: The equations for $\lambda_l(PD_{1..n}-PR_{1..n})$ (20) and $\frac{\partial\,\lambda_l}{\partial\ \left(PD_n-PR_n\right)}$ (25) can be now fed into the NBT constraint (17) to determine the threshold point at every bus. Because the NBT constraint (17) is embedded directly in the OPF, the threshold DR at every bus is co-optimized. In other words, the threshold DR quantity for every bus is determined for all buses simultaneously. This is important because changes in DR at one bus can affect the threshold DR at other buses, so the thresholds cannot be accurately calculated in isolation outside the OPF.

REFERENCES

[1] Federal Energy Regulatory Commission, "Reports on demand response and advanced metering." [Online]. Available: https://www.ferc.gov/industries/electric/indus-act/demand-response/dem-res-adv-metering.asp. Accessed: Jun. 6, 2017.

[2] M. H. Albadi and E. F. El-Saadany, "Demand response in electricity markets: An overview," in *Proc. IEEE Power Eng. Soc. Gen. Meeting*, 2007, pp. 1–5.

[3] M. P. Moghaddam, A. Abdollahi, and M. Rashidinejad, "Flexible demand response programs modeling in competitive electricity markets," *Appl. Energy*, vol. 88, no. 9, pp. 3257–3269, 2011.

[4] R. Alasseri, T. J. Rao, and K. J. Sreekanth, "Conceptual framework for introducing incentive-based demand response programs for retail electricity markets," *Energy Strateg. Rev.*, vol. 19, pp. 44–62, 2018.

[5] J. S. Vardakas, N. Zorba, and C. V. Verikoukis, "A survey on demand response programs in smart grids: Pricing methods and optimization algorithms," *IEEE Commun. Surv. Tut.*, vol. 17, no. 1, pp. 152–178, Jan.–Mar. 2015.

[6] Federal Energy Regulatory Commission, "Order 745 demand response compensation in organized wholesale energy markets," 2011. [Online]. Available: https://www.ferc.gov/EventCalendar/Files/20110315105757-RM10-17-000.pdf. Accessed: Sep. 30, 2015.

[7] L. Xu, "Demand response net benefit test," *California Independent System Operator, Market Analysis Development*, 2011. [Online]. Available: https://www.caiso.com/Documents/FinalProposal_Appendix-DemandResponseNetBenefitsTest.pdf. Accessed: Aug. 31, 2017.

[8] MISO, "Net benefits test for demand response compenstion update," 2012. [Online]. Available: https://www.misoenergy.org/Library/Repository/Report/Demand Response/Net Benefits Analysis Report.pdf. Accessed: Aug. 31, 2017.

[9] CAISO, "Demand response net benefits test results." [Online]. Available: https://www.caiso.com/Pages/documentsbygroup.aspx?GroupID = AA4CD173-9624-4B52-B148-3D3C8EAB375C. Accessed: Feb. 7, 2020.

[10] PJM Interconnection, "Net benefit test results," [Online]. Available: https://www.pjm.com/-/media/markets-ops/demand-response/net-benefits/net-benefits-historical-results.ashx?la = en. Accessed: Feb. 7, 2020.

[11] ISO New England, "Demand response threshold price summary," [Online]. Available: https://www.iso-ne.com/isoexpress/web/reports/pricing/-/tree/demand-response-threshold-price-summary. Accessed: Feb. 7, 2020.

[12] A. I. Negash and D. S. Kirschen, "Optimizing demand response price and quantity in wholesale markets," in *Proc. IEEE Power Energy Soc. Generation Meeting*, 2014.

[13] D. H. Vu, K. M. Muttaqi, A. P. Agalgaonkar, and A. Bouzerdoum, "Customer reward-based demand response program to improve demand elasticity and minimise financial risk during price spikes," *IET Generation Transmiss. Distrib.*, vol. 12, no. 15, pp. 3764–3771, 2018.

[14] M. Parvania, M. Fotuhi-Firuzabad, and M. Shahidehpour, "ISO's optimal strategies for scheduling the hourly demand response in day-ahead markets," *IEEE Trans. Power Syst.*, vol. 29, no. 6, pp. 2636–2645, Nov. 2014.

[15] W. A. Bukhsh, C. Zhang, and P. Pinson, "An integrated multiperiod OPF model with demand response and renewable generation uncertainty," *IEEE Trans. Smart Grid*, vol. 7, no. 3, pp. 1495–1503, May 2016.

[16] E. Mahboubi Moghaddam, M. Nayeripour, J. Aghaei, A. Khodaei, and E. Waffenschmidt, "Interactive robust model for energy service providers integrating demand response programs in wholesale markets," *IEEE Trans. Smart Grid*, vol. 9, no. 99, Jul. 2016.

[17] K. Kopsidas, A. Kapetanaki, and V. Levi, "Optimal demand response scheduling with real-time thermal ratings of overhead lines for improved network reliability," *IEEE Trans. Smart Grid*, vol. 8, no. 6, pp. 2813–2825, Nov. 2017.

[18] N. G. Paterakis, M. Gibescu, A. G. Bakirtzis, and J. P. S. Catalao, "A multi-objective optimization approach to risk-constrained energy and reserve procurement using demand response," *IEEE Trans. Power Syst.*, vol. 33, no. 4, pp. 3940–3954, Jul. 2018.

[19] C. Zhao, J. Wang, J. P. Watson, and Y. Guan, "Multi-stage robust unit commitment considering wind and demand response uncertainties," *IEEE Trans. Power Syst.*, vol. 28, no. 3, pp. 2708–2717, Aug. 2013.

[20] N. Padmanabhan, M. Ahmed, and K. Bhattacharya, "Simultaneous procurement of demand response provisions in energy and spinning reserve markets," *IEEE Trans. Power Syst.*, vol. 33, no. 5, pp. 4667–4682, Sep. 2018.

[21] J. Ma and B. Venkatesh, "Demand response procurement framework: A new four-step probabilistic method," *IET Generation Transmiss. Distrib.*, vol. 14, pp. 606–618, 2019.
[22] J. Ma and B. Venkatesh, "A new measure to evaluate demand response effectiveness and its optimization," *Elect. Power Syst. Res.*, vol. 182, 2020.
[23] Southwest Power Pool, "Net benefits test documentation and history," 2012. [Online]. Available: https://www.spp.org/documents/31617/net benefits test documentation and history.pdf. Accessed: Aug. 30, 2017.
[24] Independent Electricity System Operator, "Ontario's internal zones, internal interfaces and external interconnections," [Online]. Available: http://www.ieso.ca/-/media/files/ieso/power-data/data-directory/areainterface_defn_10zones.pdf?la = en. Accessed: Jun. 10, 2019.
[25] Independent Electricity System Operator, "Zonal demands," 2018. [Online]. Available: http://reports.ieso.ca/public/DemandZonal/PUB_DemandZonal_2018.csv. Accessed: Jun. 7, 2019.
[26] Independent Electricity System Operator, "Monthly generator output and capability data," 2019. [Online]. Available: http://reports-qa.ieso.ca/public/GenOutputCapabilityMonth/. Accessed: Jun. 3, 2019.
[27] PJM, "Daily energy market offer data," [Online]. Available: http://www.pjm.com/markets-and-operations/energy/real-time/historical-bid-data/unit-bid.aspx. Accessed: Jun. 26, 2018.
[28] MATLAB, "Adaptwb," [Online]. Available: https://www.mathworks.com/help/deeplearning/ref/adaptwb.html. Accessed: Jun. 25, 2020.
[29] MATLAB, "Neural net fitting app." 2019.

Jessie Ma (Member, IEEE) received the B.A.Sc. degree from the University of Toronto, Toronto, ON, Canada, in 2001 and the M.P.A. degree from the Harvard Kennedy School, Cambridge, MA, USA, in 2009. She is currently working toward the Ph.D. degree with Ryerson University, Toronto, ON, Canada. She is currently a Research Fellow with the Centre for Urban Energy, Ryerson University. She has had a decade of utility experience at Hydro One in both technical and corporate roles. Her research interests are in power systems economics and optimization.

Bala Venkatesh (Senior Member, IEEE) received the Ph.D. degree from Anna University, Chennai, India, in 2000. He is currently a Professor and Academic Director of the Centre for Urban Energy, Ryerson University, Toronto, ON, Canada. His research interests are power system analysis and optimization.